Colloids and Surfaces B: Biointerfaces 88 (2011) 78–84

Contents lists available at ScienceDirect

Colloids and Surfaces B: Biointerfaces

journal homepage: www.elsevier.com/locate/colsurfb

Novel polyurethane ionomer nanoparticles displayed a good biosensor effection

Wenbo Zhao [a], Guohui Zhang [a], Lancao Jiang [a], Tianhong Lu [a], Xiaohua Huang [a,*], Jian Shen [a,b,**]

[a] Jiangsu Key Laboratory of Biofunctional Materials, College of Chemistry and Materials Science Nanjing Normal University, Nanjing 210046, PR China
[b] Research Center of Surface and Interface Chemistry and Engineering Technology, School of Chemistry and Chemical Engineering, Nanjing University, Nanjing 210093, PR China

ARTICLE INFO

Article history:
Received 11 March 2011
Received in revised form 7 June 2011
Accepted 8 June 2011
Available online 6 July 2011

Keywords:
Polyurethane ionomer nanoparticles
Hemoglobin
Biosensor
Electrocatalysis

ABSTRACT

This study described the bioelectrochemistry property of hemoglobin (Hb) on biopolymer film of polyurethane ionomer nanoparticles (PUI-NPs) noncovalently functionalized with multiwall carbon nanotubes (MWCNTs). The polyurethane ionomer nanoparticles (PUI-NPs) were synthesized by emulsion polymerization, and could provide a good biocompatible microenvironment for Hb immobilization. The characteristic of (PUI-NPs)/MWCNTs and Hb/(PUI-NPs)/MWCNTs composite films were performed by using transmission electron microscopy (TEM), scanning electron microscopy (SEM), Fourier transform infrared (FT-IR) spectroscopy and circular dichroism (CD). Analytical results indicated that the immobilized Hb could maintain its native conformation in the (PUI-NPs)/MWCNTs hybrid film. Entrapped Hb in (PUI-NPs)/MWCNTs preserved its bioactivities and exhibited an excellent electrochemical behavior with a formal potential of −0.346 V in a pH 7.0 phosphate buffer. The formal potential of Hb varied linearly with the increase of pH in the range of 5.0–9.0 with a slope of 52.9 mV pH^{-1}, indicating that one proton participated in the electrochemical reaction process. Moreover, the resulting biosensor displays an electrocatalytic activity to hydrogen peroxide (H_2O_2). The linear range for the determination of H_2O_2 was from 6.5×10^{-7} to 8.0×10^{-5} M with a detection limit of 2.4×10^{-7} M and a Michaelis–Menten constant K_m^{app} value of 0.155 mM. Consequently, our investigation demonstrated that the proposed method opens a way to develop biosensors by using polymer with good biocompatible in its nanostructured information.

1. Introduction

In recent years, nanotechnology has become one of the most exciting fields in analytical chemistry. Many kinds of nanoparticles have been used to construct novel sensing devices, especially electrochemical sensors and biosensors [1]. For example, noble metals such as Au, Ag and Pt nanoparticles, in particular Au nanoparticles, have been used to immobilize several kinds of proteins and further fabricated the different electrodes. Owing to their biocompatibility and catalytic properties, the prepared electrodes retained the proteinic activity and can get the higher enhancement of electron transfer [2–9]. Some nonmetal nanoparticles, such as oxide nanoparticles TiO_2, SiO_2, Fe_3O_4, ZrO_2 and Co_3O_4 can also enhance the electron transfer between proteins and electrodes in certain systems [10–15]. Semiconductor nanoparticles such as CdS, PbS were often employed as labels in biosensors [16–18]. Most recently, the polymer matrixes for immobilization of proteins on biosensing became a promising way to exploiting their application foreground in electroanalysis. These polymers include polypyrrole [19,20], polyaniline [21,22], polyacrylonitrile [23], chitosan [24,25,11] and even some block copolymers [26,27] etc. However, there are still few studies concerning polymer nanoparticles for immobilization of proteins on electrode surface. Nanostructured polymers being identified as very promising immobilization matrixes received much attention because of their good biocompatibility, thermal, long-term stability and multifunctions. With entrapment of protein into polymer nanoparticles, a series of novel and improved sensing devices can be constructed.

Polyurethane (PU) possesses good biocompatibility and desirable mechanical properties such as strength, abrasion resistance, and flexibility and has been widely used as cardiovascular biomaterials [28]. PU is a nonconducting polymer with low permeability and high selectivity to the interferent. The permeability can be partly enhanced by entrapping protein into the polymer film due to the varied polymer morphology [29]. In the present work, a PU film composed of nanoparticles is achieved and mixed with multiwalled carbon nanotubes (MWCNTs) for studying the immobilization and the direct electron transfer of redox proteins.

Carbon nanotubes (CNTs) have been extensively investigated for electroanalytical applications due to their unique structure and physical properties. The excellent electrical conductivity, large surface area, surface chemical flexibility and ideal porous structure

* Corresponding author. Tel.: +86 25 85891651; fax: +86 25 83598280.
** Corresponding author. Tel.: +86 25 83594933; fax: +86 25 83594404.
E-mail addresses: wxxhhuang@yahoo.com (X. Huang), jshen@njnu.edu.cn (J. Shen).

0927-7765/$ – see front matter © 2011 Elsevier B.V. All rights reserved.
doi:10.1016/j.colsurfb.2011.06.011

make CNTs attractive materials for electroanalysis [30]. Incorporation of polymer nanoparticles with CNTs will lead to new composite materials possessing the properties of each component, or even with a synergistic effect [31], which would be useful in the fields of biotechnology and bioanalytical chemistry. The preparation of CNTs nanocomposite materials has important implication to the development of materials for high performance electrodes and biosensors. In this paper, polyurethane ionomer nanoparticles (PUI-NPs) have been homogeneously coated on multiwalled carbon nanotubes (MWCNTs) and formed a uniformly composite film. The presence of MWCNTs provides a promising stage for the interactions of proteins and polyurethane ionomer nanoparticles, increases the three-dimensional structure for loading of biomolecules, improves the conductivity of the PUI film and accelerates the electron transfer through the conducting tunnels of MWCNTs with the immobilized proteins. Hemoglobin (Hb), probably is the most thoroughly studied protein and is an excellent mode for research on the direct electron transfer between proteins and underlying electrodes [32]. We choose Hb as a model protein for studying the direct electron-transfer behavior of the immobilized protein and (PUI-NPs)/MWCNTs composites.

In the past researches, enzyme was usually immobilized by polymeric materials film. In our case, polymeric nanoparticles were used to immobilize enzyme. Riedel et al. reported that the topology structure presented on the surface of materials could affect the absorption and activity of protein [33]. The three dimension architecture of PUI-NPs provides a significant increase in the effectiveness for Hb loading on the electrode surface, and allows the electroactive probe to easily diffuse through the films. Moreover, the good biocompatibility of PUI-NPs was also proved by our group [34]. So, here, PUI-NPs and MWCNTs were chosen to modify the GCEs for the retention of Hb's biological activity and the electron transfer between Hb and electrodes. Electrochemical behavior of the sensor was studied in detail. Direct electron transfer between Hb and glassy carbon electrode (GCE) and the electrocatalytic reduction of H_2O_2 at biosensor were observed.

2. Material and methods

2.1. Materials

4,4′ Diphenylmethane diisocyanate (MDI) from Sigma–Aldrich was stored at −22 °C before use to prevent its dimerization. Poly(tetramethylene ether glycol) (PTMG) and dimethylolpropionic acid (DMPA) from Aldrich were respectively dried in a vacuum oven for 12 h and in air for 2 h at 100 °C. Ethyl acetate and pyrrolidinone were purified and dried over 4 Å molecular sieves after distillation. 3-Aminopropyl triethoxysilane (APTES) was purchased from Sigma. Multiwalled carbon nanotubes (MWCNTs, 10–20 nm in diameter and 1–2 μm in length with a purity of more than 95%) were obtained from Shenzhen Nanotech Port Co., Ltd., and H_2O_2 (30%) was from Nanjing Chemical Plant. Hemoglobin (Hb, from bovine blood, MW 66,000, lyophilized powder, the isoelectric point pI ~7.4) was purchased from Sigma (Saint Louis, MO, USA) and used without further purification. The 0.1 M phosphate buffered saline (PBS) solutions with various pH values were prepared by mixing two stock solutions of Na_2HPO_4 and NaH_2PO_4. All other chemicals were used without further purification.

2.2. Preparation of polyurethane ionomer nanoparticles

The preparation method of polyurethane ionomer nanoparticles is described as follows [34]: 4.25 g of MDI, 8.8 g of PTMG, and 0.5 μL of dibutyl tin dilaurate (DBTL) were dissolved in 40 mL of ethyl acetate and added to a 500 mL four-necked round bottom flask equipped under mechanical stirring at 75 °C and a nitrogen atmosphere. Then, 0.88 g of DMPA dissolved in 10 mL of pyrrolidinone was gradually added under stirring. 4 h later, 3 mL of isopropanol was added as the end-capping agent. The solution mixture was further stirred at 40 °C for 30 min. Subsequently, 1 mL of triethylamine was added and stirred for a further 10 min. The solution mixture was divided into two parts. One part was added to a 50 mL mixture of water and sodium dodecyl sulfate (SDS) with a weight ratio of 96:4 under stirring, resulting in a white emulsion after 30 min, which was redispersed in 0.2 M phosphate buffered solution (PBS) (pH 7) under ultrasonic agitation for 30 min. The volume ratio of emulsion PU and PBS is 1:10. The PUI-NPs were purified by dialysis (Spectra/Por CE, MWCO = 10,000) in distilled water over a 7 day period to remove unreacted monomers, SDS, and salts. Finally, all the solvents were removed by freeze-drying, leading to PUI-NPs in a white powder form. The PUI-NPs obtained can be redispersed in water to form a dispersion solution.

2.3. Preparation of modified electrodes

The glassy carbon electrode (GCE) of 3 mm diameter (CH instrument, Inc., USA) was first polished to a mirror-like with 0.3 and 0.05 μm Al_2O_3 slurry on a polish cloth, rinsed with double-distilled water, and sonicated in ethanol and double-distilled water for 5 min, respectively, then allowed to dry at room temperature before use. Preparing Hb/(PUI-NPs)/MWCNTs/GCE modified electrode is as shown in Scheme 1. First, a cleaned GCE electrode was immersed in an ethanol solution of 1% (v/v) APTES for 30 min at 25 °C, rinsed five times in ethanol with sonication, and dried in air [35]. Equal amount of 5 mg mL^{-1} MWCNTs solution in DMF and 20 mg mL^{-1} PUI-NPs solution were hand-mixed thoroughly, 8 μL of resulting mixture was dropped on the silanized GCE surface and allowed to dry at room temperature for 5 h. And then 8 μL of 5 mg mL^{-1} Hb solution in H_2O was dropped on this nanocomposites surface and allowed to dry at 4 °C for 24 h. So that Hb immobilized on PUI-NPs to form Hb/(PUI-NPs)/MWCNTs/GCE [36]. The same modified method was used for Hb/(PUI-NPs)/GCE. The above prepared Hb/(PUI-NPs)/MWCNTs/GCE, Hb/(PUI-NPs)/GCE electrode were rinsed with doubly distilled water and kept in PBS at 4 °C prior to electrochemical measurements.

2.4. Electrochemical measurements

The three-electrode system consisted of a Hb/(PUI-NPs)/MWCNTs modified electrode as working electrode, a saturated calomel electrode (SCE) as reference electrode and a platinum wire as auxiliary electrode. Buffers were purged with highly purified nitrogen for at least 15 min and maintained under nitrogen atmosphere during electrochemical process. All the electrochemical measurements were performed on a CHI760C electrochemistry workstation (CH Instruments). Cyclic voltammetric measurements were done in an unstirred electrochemical

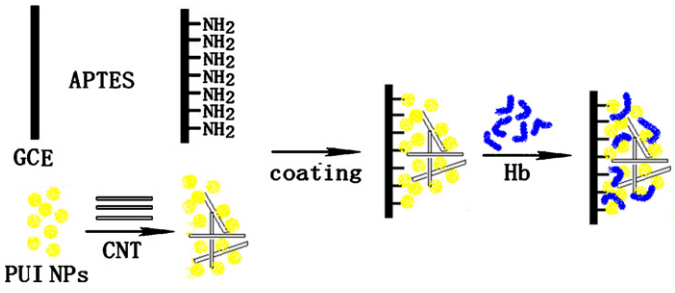

Scheme 1. Preparation process of the Hb/(PUI-NPs)/MWCNTs/GCE modified electrode.

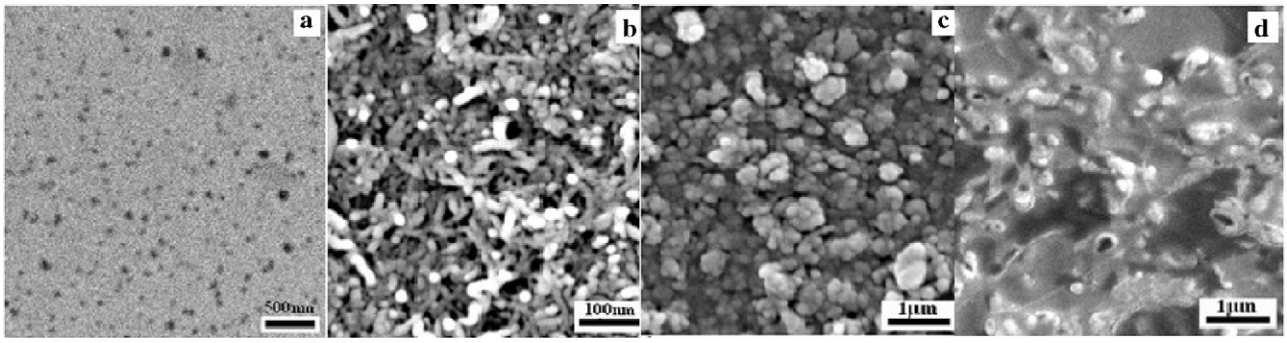

Fig. 1. TEM and SEM images of (a) PUI-NPs, (b) MWCNTs, (c) (PUI-NPs)/MWCNTs and (d) Hb/(PUI-NPs)/MWCNTs films on mica slices.

cell. The amperometric measurements were performed in a stirred cell with successive additions of some volume of H_2O_2 solution into the buffer solution.

2.5. Fourier transform infrared measurements

Fourier Transform Infrared (FTIR) spectra were recorded on the Cary 5000 spectrometer from VARIAN Company. The assembling procedure of PUI-NPs, (PUI-NPs)/MWCNTs and Hb/(PUI-NPs)/MWCNTs films were performed on the clean mica slides. First, the PUI-NPs, (PUI-NPs)/MWCNTs and Hb/(PUI-NPs)/MWCNTs solution were casted on the mica slice respectively, after being dried at 4 °C, the membrane on the slides were used for FTIR measurements.

2.6. The circular dicroism (CD) spectroscopy measurements

The circular dicroism (CD) spectra of the Hb solutions without and with the PUI-NPs were measured over the wavelength region at the far-UV (185–260 nm) and Soret band regions (340–480 nm) in a JASCO J-715 pectropolarimeter using quartz cell with 0.2 cm path length. Each spectrum was obtained from the average result of eight scans by collecting data at 0.5 nm intervals with an integration time of 0.5 s. The secondary structure content were analyzed using the SSE-338 program provide by JASCO Co. in terms of Yongli et al. [37–39].

2.7. Transmission electron microscopy (TEM) and scanning electron microscopy (SEM) analysis

TEM image of PUI-NPs was measured by JEOL JEM 2011 interface high-resolution transmission electron microscopy. The surface of the MWCNTs, (PUI-NPs)/MWCNTs and Hb/(PUI-NPs)/MWCNTs films were observed with a SEM (JSM Model 6300 Scanning electronic microscopy, JOEL, Japan) following gold-sputtering on the film surface.

3. Results and discussion

3.1. Preparation and characterization of the PUI nanoparticles

Transmission electron microscope (TEM) image of PUI-NPs presented in Fig. 1a showed that the PUI-NPs are consisted of monodispersed elliptic nanoparticles with the average diameter of 50 nm. The morphological character of the Hb/(PUI-NPs)/MWCNTs complex nanomaterials is investigated by using scanning electron microscopy (Fig. 1b–d). As shown in image b, the MWCNTs are intertwined noncovalently with each other into a complex three-dimensional (3D) architecture. After the PUI nanoparticles mixed with MWCNTs, nanoparticles could be found immobilizing onto the surface of the nanotube of the MWCNTs (image c). The addition of Hb changes the structure of the (PUI-NPs)/MWCNTs film and forming a porous distributed film. Thus, PUI-NPs film on the surface of MWCNTs could prevent MWCNTs to contact with Hb directly and provide a friendly microenvironment to retain its bioactivity of the immobilized Hb.

The properties of the resulting PUI, PUI-MWCNTs, Hb and PUI-Hb-MWCNTs films are characterized with FTIR spectra. The characteristic amide I and amide II bands of proteins provide detailed information on the secondary structure of the polypeptide chain [40]. In Fig. 2, curves a and b, the absorption bands (1700–1600 cm^{-1}) on IR spectrum of PUI film and Hb molecules attributed to the stretching vibration of the C=O of amide in PUI-NPs and the amide I stretching vibration band of the C=O of the peptide linkages in the protein's backbone, respectively. The amide II band (1620–1500 cm^{-1}) results from the combination of N–H banding and C–N stretching in Hb. In comparison to the curve a and b, the spectra of the amide I and II bands of Hb in the Hb/(PUI-NPs) and PUI-Hb-MWCNTs film (1652 and 1540 cm^{-1}) in curve c and d are nearly the same position and stronger than those obtained for native Hb (1651 and 1540 cm^{-1}). The strong peak is due to the overlapping of the absorption band of the C=O stretching vibration in PUI-NPs and Hb molecules. The results suggested interaction between polyurethane and protein. However, the interaction does not destroy the structure and properties of the Hb in the film. Therefore, it can be concluded that Hb molecules have retained their natural heme secondary structure in the nanocomposite systems.

It was reported that CD is one of the most sensitive physical techniques for determining the secondary structures and monitoring the structural changes of biomacromolecules [38]. Fig. 3A represents the CD spectra of Hb in PBS without and with PUI-NPs in the far-UV region. In the absence of PUI-NPs, a positive band at 195 nm is corresponded to the π–π^* transition of the amide groups in the

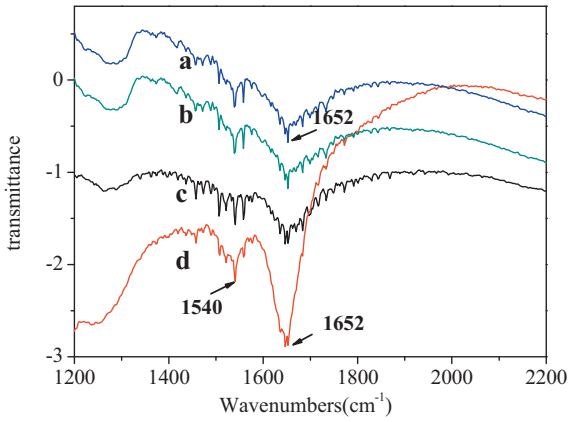

Fig. 2. FTIR spectra of (a) PUI-NPs, (b) Hb, (c) Hb/(PUI-NPs), and (d) Hb/(PUI-NPs)/MWCNTs films.

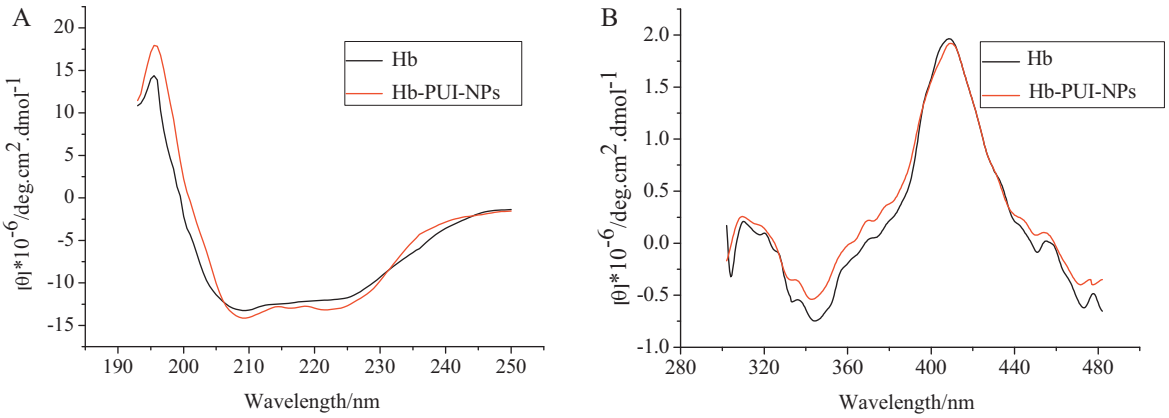

Fig. 3. (A) The CD spectra of the Hb solutions without (a) and with (b) the PUI-NPs over the wavelength region at the far-UV (190–250 nm). (B) The CD spectra of the Hb solutions without (a) and with (b) the PUI-NPs over the Soret band regions (340–480 nm).

Table 1
Comparison of the responses of some amperometric Hb sensors constructed based on different modified electrode materials.

Electrode materials	Response time (s)	Detection limit (μM)	Linear range (μM)	Ref.
HZMS-SA	–	0.6	1.75–4900	[50]
Grapheme-chitosan	–	0.51	6.5–230	[51]
Flowerlike NiO	–	0.68	2.0–1050	[52]
CuO NWBs	–	3.3	10–90	[53]
Nafion/CuS	–	4.0	8.0–700	[54]
This work	<5	0.24	0.65–80	–

peptide chain of Hb and two distinct negative bands at around 208 and 222 nm are attributed to the π–π*and *n*–π* amide transition of the peptide chain of Hb, respectively. Two peaks come from α-helix of enzyme. In the presence of PUI-NPs, the intensity of the positive band at 195 nm is obviously increased compared with that of no nanoparticles, indicating that there is a interaction between the amino acid residues in the peptide of Hb molecule and PUI-NPs, while the molar ellipticity of the two negative bands at 208 and 222 nm are lightly decreased, suggesting that the secondary structure of Hb is not obviously changed comparing with that of Hb in the absence of PUI-NPs. The data of the secondary structure of Hb calculated from the CD spectra were listed in Table 1. It was found from Table 1 that the content of α-helix and β-sheet conformation are increased about 1.5% and 1.1%, respectively; while the contents of β-turn and random coil are decreased about 0.7% and 1.9% comparing with that of Hb in the absence of PUI-NPs. These results further proved that PUI-NPs could basically maintain the native conformation of Hb, and indeed PUI-NPs have the excellent biocompatibility.

Fig. 3B shows the CD spectra of 6.39×10^{-4} M Hb in PBS without and with 4.8×10^{-4} M PUI-NPs in the far-UV Soret region. It can be observed from Fig. 3B that the Soret band at 408 nm is slightly red-shifted to 409 nm and the intensity is decreased by 1.2%. The red shift and the decrease in the intensity of the Soret band suggested that the planarity and π–π* transition energy of the porphyrin cycle in the heme group is not obviously changed [37]. In fact, the porphyrin cycle of Hb is deeply buried in the peptide of Hb, and thus, PUI-NPs unlikely interact with the porphyrin cycle of Hb directly. The possible way is that PUI-NPs interact with the amino acid residues in the peptide of Hb and then Hb undergoes an unfolding/folding process, which causes the change in the planarity of the porphyrin cycle in the heme group and influence in the exposure extent of the active center, Fe (III), in the heme group, resulting in the decrease/increase in the bioactivity of Hb. Therefore, the preservation of the native conformation of an enzyme is essential for the bioactivity [41]. The results from Fig. 3B indicated that PUI-NPs can not cause the structure of the active center in Hb molecule although there is an interaction between polyurethane ionomer and the amino acid residues in the peptide of Hb protein (Fig. 3A). It was found that polyurethane ionomer possesses COO^-, HNR^+ groups [42,43] and has the similar structure with the amino acid residues in the peptide of Hb protein. Therefore, the interac-

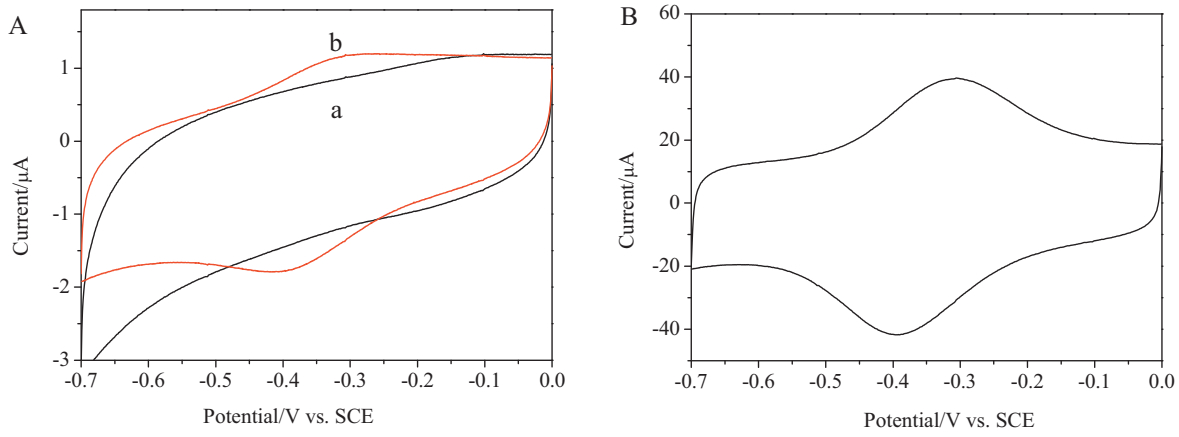

Fig. 4. (A) Cyclic voltammograms of (a) (PUI-NPs)/GCE, (b) Hb/(PUI-NPs)/GCE in 0.1 M with pH 7.0 PBS at 100 mV s^{-1} and (B) cyclic voltammograms of Hb/(PUI-NPs)/MWCNTs/GCE in 0.1 M with pH 7.0 PBS at 100 mV s^{-1}.

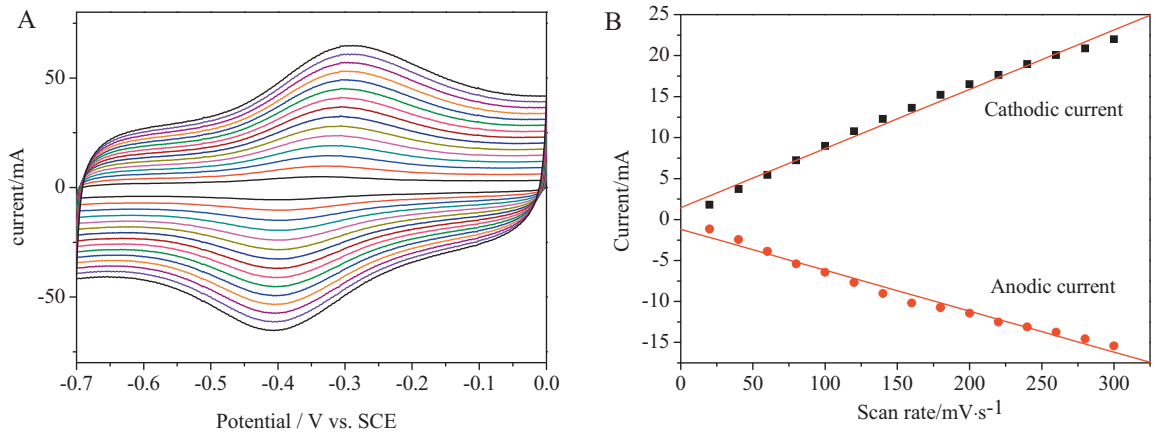

Fig. 5. (A) Cyclic voltammograms (CVs) obtained at Hb/(PUI-NPs)/MWCNTs/GCE electrode in 0.1 M with pH 7.0 PBS buffer at 20, 40, 60, 80, 100, 120, 140, 160, 180, 200, 220, 240, 260, 280 and 300 mV s^{-1} (from inner to outer). (B) Showed a plot of cathodic and anodic peak currents against potential scan rate.

tion above does not destroy the structure and properties of the Hb in the film. It can be concluded that the secondary structure of Hb molecules in the nanocomposite systems have been maintained.

3.2. Direct electron transfer of the enzyme electrode

Fig. 4 shows the cyclic voltammograms (CVs) of Hb on the PUI-NPs and MWCNTs modified GCE electrode in PBS 7.0 at 100 mV s^{-1}, respectively. The steady state of CV for PUI-NPs and Hb/(PUI-NPs) films were shown in Fig. 4A (a and b). No voltammetric signal was observed at PUI-NPs film electrode in the range of −0.7 to 0 V vs. SCE. Only when Hb was embedded in the matrix containing the nanocomposite, a pair of quasi-reversible reduction–oxidation peaks could be observed with a formal potential ($E^{\circ\prime}$) at about −0.346 V vs. SCE for both Hb-nanocomposite films. The peaks were located at the potential characteristic of heme Fe^{3+}/Fe^{2+} redox couples of the proteins [44]. When using Hb/(PUI-NPs) film as modified electrode, a pair of redox peak potentials are at −0.306 and −0.395 V. Using Hb/(PUI-NPs)/MWCNTs film as modified electrode in Fig. 4B, a pair of redox peak potentials are at −0.28 and −0.412 V, respectively. In comparison with Hb/(PUI-NPs) film electrode, the current of the redox peaks at Hb/(PUI-NPs)/MWCNTs film were much larger. The biosensor based on the nanocomposite showed very stable electrochemical responses even after 500 cycles measurements, which made it suitable for further investigations and applications.

Fig. 5 shows the cyclic voltammograms of the Hb/(PUI-NPs)/MWCNTs/GCE electrode in PBS (pH 7.0) with the scan rate varied from 20 to 300 mV s^{-1}. The obtained cathodic and anodic peak currents show a linear relationship with scan rate increasing. This revealed that the electron transfer between Hb and GC electrode was a surface-controlled electrochemical process for the immobilized Hb. The surface concentration of electroactive Hb (Γ^*) was estimated from integration of the reduction peaks in the CVs according to the following equation [45]:

$$Q = nFAI* \quad (1)$$

where Q is the charge involved the reaction, n is the number of electron transferred, F is the Faraday's constant, and A is the effective area of the GC electrode. For charge (Q) values by integration of the reduction peaks were nearly constant in the range of scan rates from 20 to 300 mV s^{-1}, the surface concentration of electroactive Hb (Γ^*) for Hb/(PUI-NPs)/MWCNTs/GCE electrode was constant with an average value of 1.82×10^{-10} mol cm^{-2}. The average peak-to-peak separations of the cyclic voltammograms (ΔE_p) of the Hb/(PUI-NPs)/MWCNTs/GCE electrode at the range of scan rate from 20 to 300 mV s^{-1} is smaller than 200 mV. The electron transfer rate constant (k_s) of Hb on the modified electrode is estimated according to the model of Laviron with the formula $k_s = mnF\upsilon/RT$ [46], where m is a parameter related to the peak-to-peak separation. The k_s value was calculated to be 1.17 s^{-1} at the scan rate of 100 mV s^{-1}, which is higher than 0.95 s^{-1} for Hb immobilized on diazonium-functionalized aligned carbon nanotubes film [47], or comparable to two times that of Hb immobilized in a poly(acrylonitrile-co-acrylic acid) film of 0.58 s^{-1} [27]. Thus,

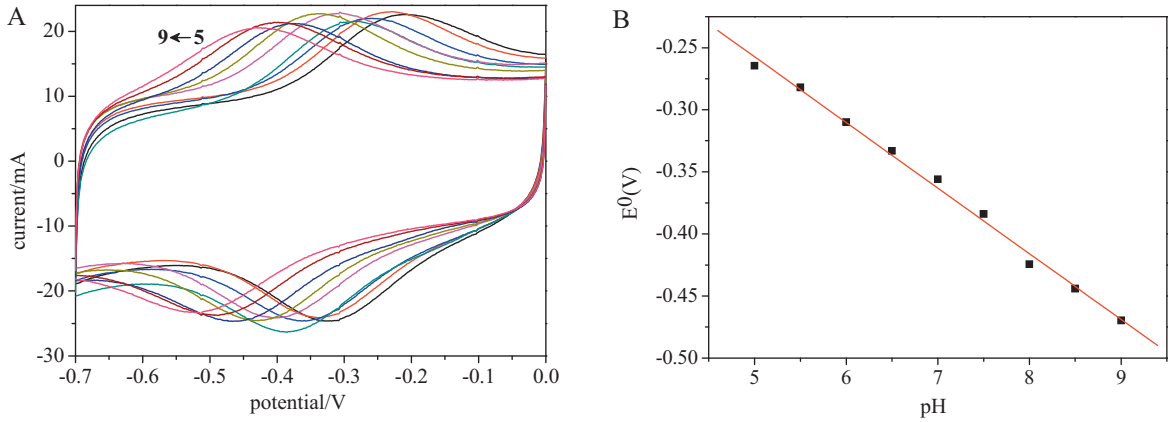

Fig. 6. (A) CVs of Hb/(PUI-NPs)/MWCNTs/GCE in 0.1 M PBS at different pH values of 5.0, 5.5, 6.0, 6.5, 7.0, 7.5, 8.0, 8.5 and 9.0 with scan rate is 0.1 V s^{-1}. (B) Plot of Hb formal potential vs. pH value.

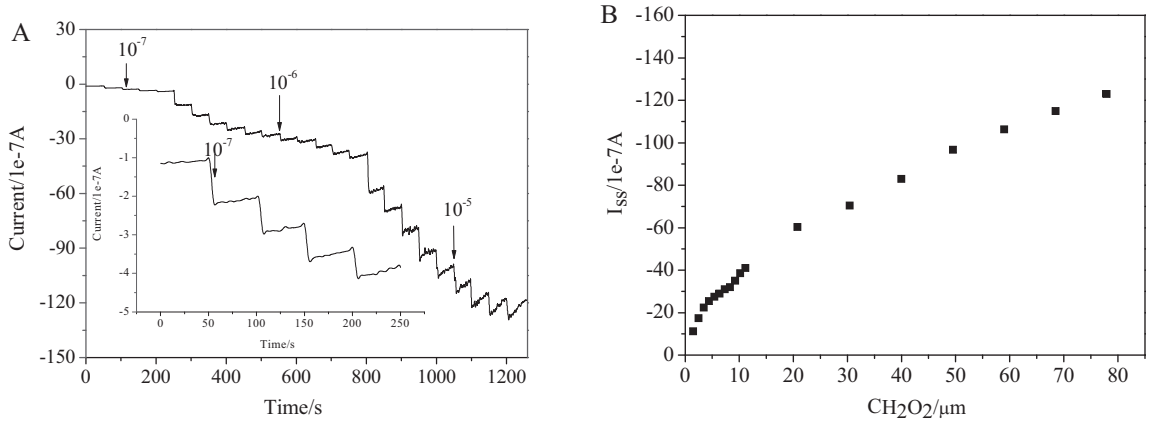

Fig. 7. (A) Dynamic response of the H_2O_2 biosensor to successive addition different concentration of H_2O_2 in the solution at the applied potential of −0.346 V. Insert was the response of the biosensor to 1.0×10^{-7} M H_2O_2. (B) Calibration plot between current and H_2O_2 concentration. Inset was the magnified part of the calibration curve.

PU-NPs can provide a microenvironment for Hb to undergo facile electron transfer reaction.

In most cases, the solution pH is essential to the electrochemical behaviors of proteins. Generally, the $E^{\circ\prime}$ of the redox couple depends on solution pH which indicates the participation of proton in the redox process. Cyclic voltammograms of Hb/(PUI-NPs)/MWCNTs/GCE show a strong dependence on the pH of buffer solution, as shown in Fig. 6. Stable and well-defined cyclic voltammograms can always be obtained in the pH range from 5.0 to 9.0. Negative shifts in both cathodic and anodic peak potentials are observed with an increase in solution pH. Plot of the formal potential vs. pH produces a line with a slope of $-52.9\,\text{mV}\,\text{pH}^{-1}$ (the correlative coefficient $R^2 = 0.9947$), which is close to the expected value of $-58.0\,\text{mV}\,\text{pH}^{-1}$, indicating the reversible one-electron transfer coupled with single-proton transportation process [48,49]. The whole process may be depicted as the following reaction:

$$\text{Hb}_{\text{heme}}\text{Fe(III)} + \text{H}^+ + e^- \leftrightarrow \text{Hb}_{\text{heme}}\text{HFe(II)} \quad (2)$$

3.3. Electrocatalysis of the enzyme electrode for hydrogen peroxide

Electrocatalytic reductions of hydrogen peroxide were examined using amperometric current–time method which is one of the most widely employed techniques for biosensor. Fig. 7 shows a typical calibration curve of the Hb/(PUI-NPs)/MWCNTs/GCE for H_2O_2 determination. The applied potential is controlled at −0.346 V vs. SCE. On Fig. 7A, a clearly defined reduction current proportional to the hydrogen peroxide concentration was observed. When H_2O_2 was added to the stirring PBS solution, the biosensor responded rapidly to the substrate. The response time (achieving 95% of the steady-state current) of the biosensor was less than 5 s. Such a rapid response can be attributed to the fast diffusion of the substrate in the composite film. The typical calibration curve of the steady state current vs. H_2O_2 concentration was shown in the inset of Fig. 7B. The responses of H_2O_2 are proportional to the H_2O_2 concentration ($R^2 = 0.9815$) from 6.5×10^{-7} to 8.0×10^{-5} M with a detection limit of 2.4×10^{-7} M (the signal to noise ratio S/N was 3). The performance of the proposed method was compared with other methods as shown in Table 1. The comparative data suggests superiority of the present sensor over some earlier reported H_2O_2 biosensors, the possible reason being that PUI-NPs prevents the MWCNTs to contact with Hb directly and provides a friendly microenvironment to retain Hb's bioactivity. In addition, the 3-dimensional architecture of PUI-NPs and MWCNTs provides a significant increase in the effectiveness for Hb loading on the electrode surface, decreases the reorganizational energy for electron transfer, and allows the electroactive probe to easily diffuse through the films.

The apparent Michaelis–Menten constant (K_m^{app}), an indicator of enzyme–substrate kinetics that shows the catalytic activity of the film electrode toward the detected substance, can be calculated using to the Lineweaver-Burk equation:

$$\frac{1}{I_{cat}} = \frac{1}{I_{max}} + \frac{K_m^{app}}{I_{max} C_{H_2O_2}} \quad (3)$$

where I_{cat} is the electrocatalytic current, I_{max} is the maximum current under saturated substrate conditions, and $C_{H_2O_2}$ is the bulk concentration of H_2O_2. In this work, K_m^{app} is 0.155 mM, which is smaller than 0.26 mM of the Hb immobilized on LBL films with MWCNTs and gold nanoparticles [55], 0.9 mM of the Hb-PAN film modified GCE [23], indicating a higher affinity to H_2O_2 and good catalytic activity of the Hb/(PUI-NPs)/MWCNTs/GCE film toward the reduction of H_2O_2.

The reproducibility of the sensor was evaluated at a H_2O_2 concentration of 0.1 mM, and the relative standard deviation was 2.56% ($n = 6$). For the inter electrode repeatability of six electrodes from the same batch, the relative standard deviation was 8.7% at a H_2O_2 concentration of 0.1 mM. The stability of the sensor was investigated. Its response remained stable after continuously detecting H_2O_2 for about 2 h. When the Hb/PUE/MWCNTs/PG electrode was not in use, it was stored in PBS in a refrigerator at 4 °C. The biosensor could retain 91% of its initial response current after storage for two weeks, demonstrating good long-term stability. Good stability may be attributed to the good biocompatibility of the nanocomposite film, which can provide a favorable microenvironment for Hb to retain its bioactivity.

4. Conclusion

We synthesized polyurethane ionomer nanoparticles (PUI-NPs) by emulsion polymerization method, and successfully combined them with MWCNTs to entrap the model protein Hb as an immobilization matrix. The results of FT-IR and CD indicated that the protein in PUI-NPs retained near-native secondary structures. Redox peak currents increased linearly with the increase of scan rate, indicating a surface-controlled electrode process. The apparent heterogeneous electron-transfer rate constant (k_s) of Hb was found to be $1.17\,\text{s}^{-1}$ based on Laviron's formulism. In addition, the Hb immobilized in the (PUI-NPs)/MWCNTs films displayed excellent eletrocatalytical activity to the reduction of hydrogen peroxide with a Michaelis–Menten constant (K_m^{app}) of 0.155 mM. This mate-

rial can provide a favorable microenvironment for redox proteins and enzymes, and thus it is expected to have widely potential applications in direct electrochemistry, biosensors and biocatalysis.

Acknowledgements

This work was supported by National Natural Science Foundation of China (Grant 20874047, 21075065), the Natural Science Key Basic Research Foundation of the Jiangsu Higher Education Institutions of China (Grants 08KJA430003), the Priming Scientific Research Foundation for the High-caliber Personnel in Nanjing Normal University (Grant No. 2010103XGQ0087), and a Project Funded by the Priority Academic Program Development of Jiangsu Higher Education Institutions.

References

[1] X.L. Luo, A. Morrin, A.J. Killard, M.R. Smyth, Electroanalysis 18 (2006) 319.
[2] S.Q. Liu, D. Leech, H.X. Ju, Anal. Lett. 36 (2003) 1.
[3] A.L. Crumbliss, S.C. Perine, J. Stonehuerner, K.R. Tubergen, J. Zhao, R.W. Henkens, Biotechnol. Bioeng. 40 (1992) 483.
[4] Y. Xiao, H.X. Ju, H.Y. Chen, Anal. Chim. Acta 391 (1999) 73.
[5] J.B. Jia, B.Q. Wang, A.G. Wu, G.J. Cheng, Z. Li, S.J. Dong, Anal. Chem. 74 (2002) 2217.
[6] X.L. Luo, J.J. Xu, Q. Zhang, G.J. Yang, H.Y. Chen, Biosens. Bioelectron. 21 (2005) 190.
[7] F. Patolsky, T. Gabriel, I. Willner, J. Electroanal. Chem. 479 (1999) 69.
[8] Z.M. Liu, H. Wang, Y. Yang, H.F. Yang, S.Q. Hu, G.L. Shen, R.Q. Yu, Anal. Lett. 37 (2004) 1079.
[9] H.Y. Gu, A.M. Yu, H.Y. Chen, J. Electroanal. Chem. 516 (2001) 119.
[10] Y. Zhang, P.L. He, N.F. Hu, Electrochim. Acta 49 (2004) 1981.
[11] G. Zhao, J.J. Xu, H.Y. Chen, Electrochem. Commun. 8 (2006) 148.
[12] L.C. Jiang, W.D. Zhang, Electroanalysis 1 (2009) 988.
[13] G.Y. Shi, Z.Y. Sun, M.C. Liu, L. Zhang, Ye Liu, Y.H. Qu, L.T. Jin, Anal. Chem. 79 (2007) 3581.
[14] P.L. He, N.F. Hu, Electroanalysis 16 (2004) 1122.
[15] X.B. Lu, G.F. Zou, J.H. Li, J. Mater. Chem. 17 (2007) 1427.
[16] D. Wang, A.L. Rogach, F. Caruso, Nano Lett. 2 (2002) 857.
[17] S.Y. Ding, M. Jones, M.P. Tucker, J.M. Nedeljkovic, J. Wall, M.N. Simon, G. Rumbles, M.E. Himmel, Nano Lett. 3 (2003) 1581.
[18] K.E. Sapsford, I.L. Medintz, J.P. Golden, J.R. Deschamps, H.T. Uyeda, H. Mattoussi, Langmuir 20 (2004) 7720.
[19] P. Mailley, E.A. Cummings, S.C. Mailley, B.R. Eggins, E. McAdams, S. Cosnier, Anal. Chem. 75 (2003) 5422.
[20] M.R. Majidi, A. Jouyban, K.A. Zeynali, Electrochim. Acta 52 (2007) 6248.
[21] E.S. Forzani, H.Q. Zhang, L.A. Nagahara, I. Amlani, R. Tsui, N.G. Tao, Nano Lett. 4 (2004) 1785.
[22] M. Kanungo, A. Kumar, A.Q. Contractor, Anal. Chem. 75 (2003) 5673.
[23] D. Shan, S.X. Wang, D.B. Zhu, H.G. Xue, Bioelectrochemistry 71 (2007) 198.
[24] S.S. Jia, J.J. Fei, T. Tian, F.Q. Zhou, Electroanalysis 21 (2009) 1424.
[25] X.D. Zeng, W.Z. Wei, X.F. Li, J.X. Zeng, L. Wu, Bioelectrochemistry 71 (2007) 135.
[26] N.Q. Jia, Q. Lian, Z.Y. Wang, H.B. Shen, Sens. Actuators B 137 (2009) 230.
[27] D. Shan, G.X. Cheng, D.B. Zhu, H.G. Xue, S. Cosnier, S.N. Ding, Sens. Actuators B 137 (2009) 259.
[28] M.D. Lelah, S.L. Cooper (Eds.), Polyurethanes in Medicine, CRC Press, Boca Raton, FL, 1986.
[29] S.Q. Liu, B.P. Lin, X.D. Yang, Q.Q. Zhang, J. Phys. Chem. B 111 (2007) 1182.
[30] L.C. Jiang, W.D. Zhang, Electroanalysis 21 (2009) 988.
[31] H.P. Bai, X.X. Lu, G.M. Yang, Y.H. Yang, Chin. Chem. Lett. 19 (2008) 314.
[32] G.Y. Shi, Z.Y. Sun, M.C. Liu, L. Zhang, Y. Liu, Y.H. Qu, L.T. Jin, Anal. Chem. 79 (2007) 3581.
[33] M. Riedel, B. Mfller, E. Wintermantel, Biomaterials 22 (2001) 2307.
[34] C. Mao, L.C. Jiang, W.P. Luo, H.K. Liu, J.C. Bao, X.H. Huang, J. Shen, Macromolecules 42 (2009) 9366.
[35] Y. Wang, W.P. Qian, Y. Tan, S.H. Ding, H.Q. Zhang, Talanta 72 (2007) 1134.
[36] Y. Chen, B. Jin, L.R. Guo, X.J. Yang, W. Chen, G. Gu, L.M. Zheng, X.H. Xia, Chem. Eur. J. 14 (2008) 10727.
[37] L.H. Wang, A.H. Lu, T.H. Lu, X.L. Ding, X.H. Huang, Biochimie 92 (2010) 41.
[38] Y.L. Chen, X.F. Zhang, Y.D. Gong, N.M. Zhao, T.Y. Zeng, X.Q. Song, J. Colloid Interface Sci. 214 (1999) 38.
[39] S.F. Guo, Q. Zhou, T.H. Lu, X.L. Ding, X.H. Huang, J. Biol. Inorg. Chem. 13 (2008) 587.
[40] J.K. Kauppinen, D.J. Moffate, H.H. Mantsch, D.G. Lameron, Appl. Spectrosc. 35 (1981) 271.
[41] J.W. Tams, K.G. Welinder, Biochemistry 35 (1996) 7573.
[42] N.G. Wang, L.N. Zhang, Y.H. Lu, Ind. Eng. Chem. Res. 43 (2004) 3336.
[43] S.A. Madbouly, J.U. Otaigbe, A.K. Nanda, D.A. Wicks, Macromolecules 38 (2005) 4014.
[44] Q. Huang, Z. Lu, J.F. Rusling, Langmuir 12 (1996) 5472.
[45] R.W. Murray, in: A.J. Bard (Ed.), Electroanalytical Chemistry, vol. 13, Marcel Dekker, New York, 1984, pp. 191–368.
[46] E. Laviron, J. Electroanal. Chem. 100 (1979) 263.
[47] J. Yang, Y. Xu, R.Y. Zhang, Y.Z. Wang, P.G. He, Y.Z. Fang, Electroanalysis 21 (2009) 1672.
[48] A.M. Bond (Ed.), Modern Polarographic Methods in Analytical Chemistry, Marcel Dekker/CRC Press, New York, 1980.
[49] X.L. Chen, N.F. Hu, Y.H. Zeng, J.F. Rusling, J. Yang, Langmuir 15 (1999) 7022.
[50] J. Xu, C.H. Liu, Y.L. Teng, Microchim. Acta 169 (2010) 181.
[51] H.F. Xu, H. Dai, G.N. Chen, Talanta 81 (2010) 334.
[52] S.Y. Dong, P.H. Zhang, H. Liu, N. Li, T.L. Huang, Biosens. Bioelectron. 26 (2011) 4082.
[53] Y.M. Li, Q. Zhang, J.H. Li, Talanta 83 (2010) 162.
[54] W. Sun, R.F. Gao, R.J. Zhao, H.T. Zhu, K. Jiao, J. Iran. Chem. Soc. 7 (2010) 470.
[55] S.H. Chen, R. Yuan, Y.Q. Chai, L.Y. Zhang, N. Wang, X.L. Li, Biosens. Bioelectron. 22 (2007) 1268.